Electrophoretic Light Scattering, Dynamic Light Scattering, and Turbidimetry Studies of the Effect of Polymer Concentration on Complex Formation between Polyelectrolyte and Oppositely Charged Mixed Micelles

Yingjie Li and Paul L. Dubin*

Department of Chemistry, Indiana University−Purdue University, Indianapolis, Indiana 46202

Henry A. Havel and Shun L. Edwards

Biopharmaceutical Development, Eli Lilly and Company, Indianapolis, Indiana 46285

Herbert Dautzenberg

Max Planck Institute for Colloid and Interface Research, Teltow-Seehof O-1530, Germany

Received October 18, 1994; Revised Manuscript Received January 16, 1995®

ABSTRACT: Electrophoretic light scattering, dynamic light scattering, turbidity, and static light scattering were used to study complex formation between poly(dimethyldiallylammonium chloride) (PDMDAAC) and oppositely charged mixed micelles of Triton X-100 (TX100) and sodium dodecyl sulfate (SDS) in 0.4 M NaCl. Interpolymer complexes form with an increasing bulk weight ratio of PDMDAAC to TX100-SDS, W, at constant [TX100-SDS]. The turbidity, scattered light intensity, and apparent hydrodynamic radius of the complexes all reach maxima at $W \approx 0.09$. This value of W corresponds to a net charge ratio of PDMDAAC to TX100-SDS of 1:1. Electrophoretic light scattering indicates that the electrophoretic mobility of the complexes changes from negative to positive with increasing W and is close to zero around $W \sim 0.09$. However, neither precipitation nor coacervation is observed, in contrast to typical polyelectrolyte−oppositely charged surfactant systems. The results support a model for the complex wherein only a fraction of the charged residues are associated with corresponding charges on the TX100-SDS mixed micelles.

Introduction

Complex formation between polyelectrolytes and oppositely charged surfactants has been studied by a variety of techniques for both fundamental and technological reasons (for reviews, see refs 1−4). For example, the interaction of polyelectrolytes with oppositely charged micelles may serve as a model system for phenomena in polyelectrolyte−colloid systems. Related technological processes include water purification and precipitation of bacterial cells with polycations[5] and the stabilization of preceramic suspensions.[6] In the biological realm, similar phenomena are central to the immobilization of enzymes in polyelectrolyte complexes[7] and the purification of proteins by selective coacervation.[8−11] In addition, the fundamental interactions responsible for the nonspecific association of DNA with basic proteins[12] must also be identical to the ones that control the binding of charged colloids to oppositely charged polyelectrolytes.

The interaction between polyelectrolytes and oppositely charged surfactants is mainly electrostatic in nature.[1−4] This strong interaction causes the association to start at a very low surfactant concentration, commonly known as the critical aggregation concentration (cac),[13] which is usually orders of magnitude lower than the critical micelle concentration (cmc) of free surfactant. Continued addition of surfactant results in precipitation.[14−22] The maximum precipitation yield takes place when the charge ratio between the polyelectrolyte and the surfactant is around 1:1, which implies the formation of precipitate in some kind of stoichiometric manner. Depending upon the nature of the polyelectrolyte, further addition of excess surfactant may result in redissolution of the precipitate. Goddard and Hannan[15] reported an electrophoretic mobility close to zero at the ratio of polyelectrolyte to surfactant corresponding to maximum precipitation. Charge sign reversal was also observed in excess surfactant.

The precipitation of polyelectrolyte−surfactant systems at very low concentrations makes investigation of complex formation difficult. Dubin and co-workers[23−27] have shown that the interaction between a strong polyelectrolyte, e.g., poly(dimethyldiallylammonium chloride) (PDMDAAC), and sodium dodecyl sulfate (SDS) can be attenuated by incorporating SDS into mixed micelles with a nonionic surfactant, e.g., Triton X-100 (TX100). Soluble complexes could then exist even when the concentration of TX100-SDS is well above its critical micelle concentration (cmc). Therefore, a comparison of complex formation behavior in the PDMDAAC/TX100-SDS system with those systems studied in refs 14−21, as a function of the charge ratio of polyelectrolyte to surfactants, should be interesting. This paper is aimed at answering the following three questions: (1) How do the size and molar mass of PDMDAAC/TX100-SDS complexes change with the weight ratio of PDMDAAC to TX100-SDS (W) at constant [TX100] and [SDS], ranging from excess micelle to potentially excess polymer? (2) How does the electrophoretic mobility of the complexes change with W? (3) Will phase separation take place when the charge ratio of PDMDAAC to TX100-SDS is close to 1:1, as is described in the literature for other polyelectrolyte−surfactant systems?[14−16]

* To whom correspondence should be addressed.
® Abstract published in *Advance ACS Abstracts,* April 1, 1995.

0024-9297/95/2228-3098$09.00/0

Experimental Section

Materials and Solution Preparation. The PDMDAAC sample used in this study was synthesized by free-radical polymerization in aqueous solution using a cationic azo up to a conversion of 12%. Purification and isolation of the polymer were carried out by ultrafiltration with a membrane cutoff of 30 000 and freeze-drying. The purified sample has a weight-average molecular weight (M_w) of 2.6×10^5 (from static light scattering) and a number-average molecular weight (M_n) of 1.7×10^5 (from osmometry). TX100 was purchased from Aldrich and SDS from Fluka. The ionic strength was adjusted by addition of NaCl from Fisher. Milli-Q water was used throughout this work. TX100, SDS, and NaCl were used without further purification. Solutions were prepared by slow addition (under stirring) of 60 mM SDS in 0.4 M NaCl, to a solution of 40 mM TX100 and a known concentration of PDMDAAC, also in 0.4 M NaCl, up to a surfactant molar fraction $Y = [SDS]/([SDS] + [TX100]) = 0.3$, which corresponds to soluble complex formation. The solutions were stirred for at least 2 h before any measurement. Since the cmc for TX100-SDS under such conditions is expected to be less than 0.2 mM, this is a polyelectrolyte–micelle system. All experiments were done at room temperature (24 ± 1 °C).

Turbidimetry. Turbidity measurements, reported as 100 − % T, were performed at 420 nm using a Brinkmann PC800 probe colorimeter equipped with a 2-cm path length fiber optics probe at 24 ± 1 °C.

Dynamic Light Scattering. Solutions were passed through 0.45-μm filters (Life Science Products). Dynamic light scattering measurements were carried out at 90° scattering angle and at 24 ± 1 °C using a Brookhaven Instruments system equipped with a 72-channel digital correlator (BI-2030AT) and an Omnichrome air-cooled 200 mW argon-ion laser operating at a wavelength in vacuum of $\lambda_0 = 488$ nm.

In the self-beating mode of dynamic light scattering, the measured photoelectron count autocorrelation function $G^{(2)}(\tau,q)$ for a detector with a finite effective photocathode area has the form[28]

$$G^{(2)}(\tau,q) = N_s\langle n\rangle^2(1 + b|g^{(1)}(\tau,q)|^2) \quad (1)$$

where $g^{(1)}(\tau,q)$ is the first-order scattered electric field time correlation function; τ, the delay time; $\langle n\rangle$, the mean counts per sample; N_s, the total number of samples; A ($=N_s\langle n\rangle^2$), the base line; b, a spatial coherence factor depending upon the experimental setup and taken as an unknown parameter in the data fitting procedure; and $q = (4\pi n/\lambda_0)\sin(\theta/2)$, with n and θ being the refractive index of the scattering medium and the scattering angle, respectively.

For a solution of polydisperse particles, $g^{(1)}(\tau,q)$ has the form[28]

$$|g^{(1)}(\tau,q)| = \int_0^\infty G(\Gamma,q)\, e^{-(\Gamma(q)\tau)}\, d\Gamma \quad (2)$$

where $G(\Gamma,q)$ is the normalized distribution of line width Γ measured at a fixed value of q. In the present study, a CONTIN algorithm was used to obtain the average Γ of the complex mode, denoted as Γ_{av}.[29] The apparent translational diffusion coefficient, D, is related to Γ_{av} by $D = \Gamma_{av}/q^2$. The apparent hydrodynamic radius R_h can then be estimated via the Stokes–Einstein equation

$$R_h = k_B T/(6\pi\eta D) \quad (3)$$

where k_B is the Boltzmann constant, T is the absolute temperature, and η is the solvent viscosity.

Static Light Scattering. Static light scattering measurements were performed at 24 ± 1 °C and angles from 25° to 145° along with dynamic light scattering measurements on the same solutions as described above. Total intensity measurements extrapolated to $q = 0$ are presented here. A more quantitative analysis of the static light scattering results is obstructed by the change in the concentration of the uncomplexed micelle with increasing W, which makes it difficult to separate the contribution of complexes to the scattered intensity from the contribution of the excess micelles or free polymers. However, some qualitative conclusion could be drawn from the total intensity results since complexes, of large molar mass, should dominate the scattered intensity changes.

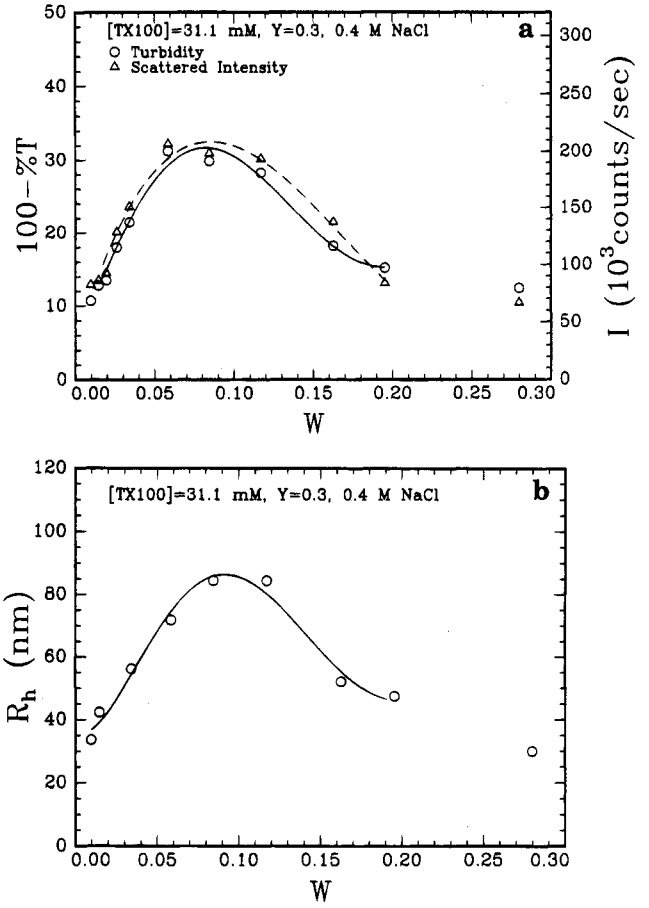

Figure 1. Turbidity, scattered intensity (a), and apparent hydrodynamic radius (dynamic light scattering) (b) of the PDMDAAC/TX100-SDS system as a function of the weight ratio of PDMDAAC to TX100-SDS. The lines are for guiding the eye only.

Electrophoretic Light Scattering. Electrophoretic light scattering was carried out at 25 ± 0.1 °C at four angles (8.6, 17.1, 25.6, 34.2°) using a DELSA 440 apparatus from Coulter Instrument Co. The electric field was applied at a constant current of 8–14 mA. The electrophoretic cell has a rectangular cross section connecting the hemispherical cavities in each electrode. The total sample volume was about 1 mL. The measured electrophoretic mobility, U, was the average value at the upper stationary layer for the four scattering angles. Further details about the electrophoretic light scattering technique can be found in ref 30.

Results and Discussion

Parts a and b of Figure 1 show the turbidity, scattered intensity, and hydrodynamic radius of the PDMDAAC/TX100-SDS system as a function of W. Despite the high turbidity, these solutions are stable with time even after 30 min of centrifugation at 4000 rpm. Thus, neither precipitation nor coacervation was observed (according to Picullel and Lindman,[31] a more descriptive term for the phenomenon of coacervation is "associative phase separation"). With W around 0.01, the system contains excess micelles. At these low W values the PDMDAAC chains must be fully saturated with micelles; we expect that only intrapolymer complexes exist. Both the turbidity and the scattered intensity show maxima with increasing W. With W around 0.01, the system contains

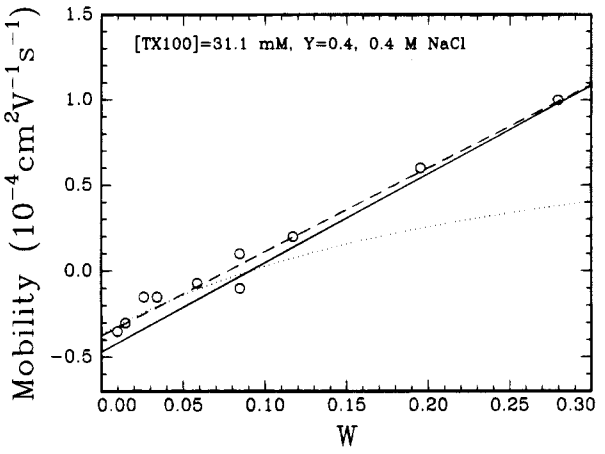

Figure 2. Electrophoretic mobility of a PDMDAAC/TX100-SDS complex as a function of the weight ratio of PDMDAAC to TX100-SDS. The two points at $W = 0.085$ correspond to a single measurement that yields a bimodal distribution. The dashed line is the best fit to eq 6 with $\beta/\alpha = 0.85$, the solid line, to eq 7, and the dotted line, to eq 10.

excess micelles.[32] The increasing turbidity and scattered intensity observed with increasing W (increasing amount of PDMDAAC at constant [TX100-SDS]) point to two possible mechanisms: (1) more complexes are formed and the amount of free micelles is decreased or (2) intrapolymer complexes could combine to form interpolymeric complexes in which two or more PDMDAAC molecules share one micelle. The results presented in parts a and b of Figure 1 cannot distinguish between these two mechanisms.

The decrease in both turbidity and scattered intensity with a further increase in W implies a decrease in the molar mass of the complexes which might be due to the breaking down of interpolymeric complexes. Since it is hard to imagine a dissociation of PDMDAAC/TX100-SDS into PDMDAAC and TX100-SDS with increasing W, the significant decrease in turbidity and scattered intensity supports the existence of interpolymer complexes when W is around 0.09.

Evidence in support of interpolymeric complexes comes from the dependence of R_h on W, as shown in Figure 1b. R_h increases from about 30 nm (twice the R_h value of micelle-free PDMDAAC) to 85 nm, with W increasing from about 0.01 to about 0.09. A further increase in W results in a decrease in R_h down to about 30 nm. Therefore, parts a and b of Figure 1 establish the formation of interpolymer complexes when W is close to 0.09, since an intrapolymer complex is not likely to have dimensions 6 times larger than the surfactant-free polymer.[27]

Further information regarding the structure of complexes may be obtained from electrophoretic mobility results, as shown in Figure 2. At low W, the complexes have a net negative charge; at very high W, the complexes bear a net positive charge. The continuous change in mobility suggests a continuous change in composition with W, implying that the binding of micelles is not highly cooperative (in a fully cooperative binding process polymer chains would be either saturated with or free from micelles). The electrophoretic mobility is very close to zero when W is close to 0.09, which corresponds to a net charge ratio of N^+ in PDMDAAC to $-OSO_3$ in TX100-SDS of 1:1. It is known that in polyelectrolyte–oppositely charged surfactant systems maximum precipitation takes place when a 1:1 charge ratio is reached,[14-16] under which conditions zero mobility has also been observed.[15] The lack of precipitation or coacervation in this PDMDAAC/TX100-SDS system is different from polyelectrolyte/surfactant systems without nonionic surfactant.[14-16]

At a point near zero mobility, the distribution of electrophoretic mobilities exhibits two peaks of opposite sign, as opposed to a single zero-mobility peak. Thus, at W very close to 0.09, the system tends to form two kinds of complexes, one with a positive charge and the other with a negative charge. One explanation is that the aggregation number of the bound mixed micelles is not variable. Although a bulk 1:1 stoichiometry can be achieved, microscopic 1:1 stoichiometry cannot be reached so exactly. From measurements of micelle aggregation number[27] we can state that 14.8 micelles per PDMDAAC molecule are needed to reach a net charge ratio of 1:1. Some complexes will be overneutralized by, say, 15 micelles and the rest underneutralized by, say, 14 micelles. Of course, this speculation may not hold if either the polyelectrolyte or micelle has a broad size distribution.

The maxima of turbidity, scattered intensity, apparent hydrodynamic radius, and the near-zero mobility at a 1:1 charge ratio may be an indication of strong electrostatic interaction between PDMDAAC and TX100-SDS so that there are very few free TX100-SDS micelles and very few free PDMDAAC macromolecules at $W \sim 0.09$, i.e., a very large binding constant. The result is that the bulk, macroscopic stoichiometry reflects the microscopic stoichiometry of complexes.

The apparent linearity of the electrophoretic mobility with W deserves further comment. The mean electrophoretic mobility of the complexes, U_x, is related to the total charge of the complexes, q_x, and the friction coefficient f_x by

$$U_x = q_x/f_x = (n_p q_p \alpha - n_m q_m \beta)/f_x \quad (4)$$

where n_p, n_m, q_p, q_m, α, and β are respectively the number of polymer chains per complex, the number of micelles per complex, the charge of PDMDAAC, the charge on the micelles, a constant to take into account the counterions accompanying PDMDAAC, and a constant to take into account the counterions accompanying the micelles. It is known that M_w of the mixed micelles is 1.9×10^5.[27] As noted in the preceding paragraph, the maxima in turbidity, scattered intensity (Figure 1a), and apparent hydrodynamic radius (Figure 1b), all at W corresponding approximately to a 1:1 charge ratio of PDMDAAC to TX100-SDS, imply that the microscopic stoichiometry might equal the bulk stoichiometry (not, of course, at very low or very high W where free micelles or free PDMDAAC may exist). Then, at least to a first-order approximation, we can relate W to n_p/n_m by $W = (M_{w,p}/M_{w,m})(n_p/n_m) = (1/0.74)(n_p/n_m)$, where $M_{w,p}$ and $M_{w,m}$ are the weight-average molecular weights of the polymer and micelles, respectively. Equation 4 can thus be written as

$$U_x = (\alpha q_p)(n_m/f_x)(0.74W - 0.067\beta/\alpha) \quad (5)$$

In eq 5 only n_m, R_h, and W are variables. A linear relation of U_x *vs* W can be obtained only if we *assume* that n_m/f_x is a constant with respect to W. Thus we have

$$U_x = K(0.74W - 0.67\beta/\alpha) \quad (6)$$

where K is an adjustable parameter. If we take β/α as

an additional adjustable parameter, we achieve the dashed line in Figure 2, for $\beta/\alpha = 0.85$. Equations 4–6 are further simplified by assuming the same counterion condensation for both PDMDAAC and TX100-SDS and setting $\beta/\alpha = 1$. Then we have

$$U_x = K(0.74W - 0.067) \tag{7}$$

in which K is the only adjustable parameter. Still, a reasonable fit results, as shown by the solid line in Figure 2.

With regard to the physical meaning of n_m/f_x = constant, we can write

$$f_x = \kappa n_m f_m \tag{8}$$

where κ is a constant, and f_m is the frictional coefficient of polymer-free micelle; this implies that the frictional coefficient of the complex is dominated by bound micelles. The polymer chains that bridge micelles contribute to f_x only through a coupling effect, and their direct contribution to f_x is not significant compared to that of bound micelles.

Another way to describe the electrophoretic mobility is to treat the complexes as free-draining particles and write the electrophoretic mobility as

$$\begin{aligned} U_x &= (\alpha n_p q_p - \beta n_m q_m)/(n_p f_p + \kappa n_m f_m) \\ &= (\alpha q_p/f_p)(0.74W - 0.067\beta/\alpha)/(0.74W + \kappa f_m/f_p) \end{aligned} \tag{9}$$

where f_p is the friction coefficients of micelle-free polymer. The introduction of the coupling factor κ into eq 9 is based on the consideration that micelles partially enveloped by PDMDAAC chains might have a different friction coefficient than free micelles. The difference between eqs 8 and 9 is that the latter adds an additional term $n_p f_p$ to the contribution of polymer chains to f_x. The electrophoretic mobility of micelle-free PDMDAAC in 0.4 M NaCl is 1.1×10^{-4} cm^2 V^{-1} s^{-1}, i.e., $U_p = \alpha q_p/f_p = 1.1 \times 10^{-4}$ cm^2 V^{-1} s^{-1}. If we take $\kappa f_m/f_p = K'$ as an adjustable parameter, eq 9 can be written as

$$U_x = (0.81W - 0.074\beta/\alpha)/(0.74 + K'')(10^{-4}\ \text{cm}^2\ \text{V}^{-1}\ \text{s}^{-1}) \tag{10}$$

Equation 10 fits the data only at low W, as shown by the dotted line in Figure 2. That is, the actual electrophoretic mobility reaches the value of a pure PDMDAAC solution more rapidly than predicted by eq 10. Therefore, it seems that a change from free-draining to non-free-draining structure might happen above $W = 0.09$. Comparison of eqs 8 and 9 with Figure 2 reveals that, above $W = 0.09$, eq 9 overestimates the contribution of polymer to f_x. More structural details cannot be offered at present.

The lack of precipitation at a 1:1 charge ratio and near-zero mobility may be explained by thermodynamic considerations. The backbone of PDMDAAC is hydrophobic; hydration of its charged moiety is the dominant reason for solubility. Similarly, favorable hydration of the charged head group of SDS provides water solubility despite the hydrophobic tail. Therefore, complex formation and the elimination of counterions will make the complexes less hydrophilic and may lead to aggregation. The electrostatic interaction between PDMDAAC and TX100-SDS is the main driving force for complex formation. This interaction increases with increasing the micellar molar fraction of SDS (Y) and decreasing the ionic strength. However, in order to maximize the formation of ion pairs between PDMDAAC residues and the micellar charge groups, adjustment of the PDMDAAC chain configuration must occur (since the spacing between charges on PDMDAAC, 0.7 nm, is so small compared to the average distance between sulfate groups in the free micelles, *ca.* 3 nm, highly efficient ion pairing is never very likely). This restriction results in a loss of chain entropy, which opposes complex formation. Complex formation, therefore, reflects a balance between these two factors, which leads to a structure in which ion-pair formation is incomplete, even when the net charge is very close to zero. In this way, the PDMDAAC molecules can largely retain their random-walk configuration while still allowing for a significant degree of electrostatic interaction. The unassociated charge is responsible for the water solubility of the complexes. Therefore, model A in Figure 3 should be a better description of the complex than model B.

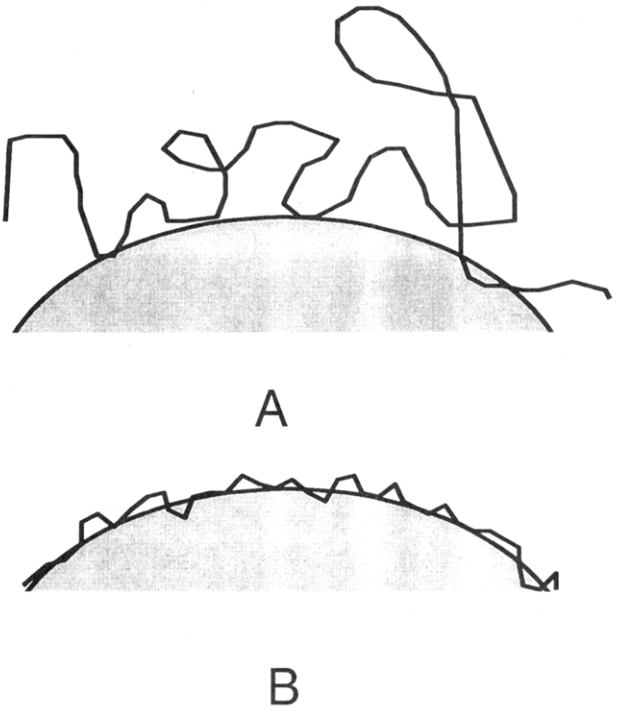

Figure 3. Schematic two-dimensional diagram of possible local PDMDAAC/TX100-SDS complex structures: (A) partially ion-paired; (B) completely ion-paired.

Parts a and b of Figure 1 indicate that interpolymer complexes tend to form when the electrophoretic mobility of complexes is close to zero. Earlier, Dubin *et al.*[25] also speculated that interpolymer complexes formed only when the intrapolymer complexes were close to electrical neutrality, in agreement with our observation. This is understood as a consequence of the decrease in the repulsive force among complexes with decreasing charge. With a further increase in W, the complexes gain a more positive charge and become more hydrophilic. The repulsive force within interpolymer complexes is also increased. The interpolymer complexes may then disaggregate into intrapolymer complexes, which may be responsible for the strong decrease in both turbidity and R_h up to $W \sim 0.17$. Above $W \sim 0.17$, a further increase in W only results in a small decrease in both turbidity and R_h. This can be explained by intrapolymer complexes in which the number of bound micelles per PDMDAAC molecule decrease with increasing W.

Conclusion

Electrophoretic light scattering, dynamic light scattering, turbidimetry, and static light scattering have been used to study PDMDAAC/TX100-SDS complex formation as a function of the bulk weight ratio of polymer:surfactant, at constant [TX100] and [SDS], and at $Y = 0.3$. With increasing PDMDAAC concentration, the turbidity, the scattered intensity, and the apparent hydrodynamic radius go through a maximum, and the electrophoretic mobility passes from negative to positive. These maxima correspond to the formation of interpolymer complexes. Such interpolymer complexes will break up with a further increase in the PDMDAAC concentration. The maxima in turbidity, scattered intensity, and hydrodynamic radius correspond to a 1:1 charge ratio of PDMDAAC to TX100-SDS. The electrophoretic mobility is close to zero at this 1:1 charge ratio.

Unlike typical polyelectrolyte–oppositely charged surfactant systems, neither precipitation nor coacervation is observed when the electrophoretic mobility is close to zero. Complex formation reflects a balance of two opposing factors: the electrostatic interaction between PDMDAAC and TX100-SDS which favors complex formation, and the entropy loss due to the restriction of PDMDAAC to some certain fixed configuration. Based in part on consideration of this entropy loss, we propose a model for PDMDAAC/TX100-SDS complexes wherein only part of the positive charge in PDMDAAC and part of the negative charge in TX100-SDS interact. The concomitant low degree of ion pairing in the complex allows for strong hydration and osmotic swelling and thus minimizes phase separation.

Acknowledgment. The support of Grant DMR9311433 from the National Science Foundation, jointly funded by the Divisions of Materials Research and Chemical and Transport Systems, is gratefully acknowledged. We thank Dr. W. Jaeger of Fraunhofer Institute for Applied Polymer Research, 14513 Teltow-Seehof, Germany, for providing the PDMDAAC sample and Vincent A. Romano and David J. Borts for experimental assistance.

References and Notes

(1) Goddard, E. D. *Colloids Surf.* **1986**, *19*, 301.
(2) Hayakawa, K.; Kwak, J. C. T. In *Cationic Surfactants. Physical Chemistry*; Rubingh, D. N., Holland, P. M., Eds; Marcel Dekker: New York, 1991; Chapter 5, p 189.
(3) Lindman, B.; Thalberg, K. In *Interactions of Surfactants with Polymers and Proteins*; Goddard, E. D., Ananthapadmanabhan, K. P., Eds.; CRC Press: Boca Raton, FL, 1993; Chapter 5.
(4) Li, Y.; Dubin, P. L. In *Rheology of Surfactant Solutions*; Herb, C. A., Prud'homme, R. K., Eds.; American Chemical Society: Washington, DC, in press.
(5) Kawabata, N.; Hayashi, T.; Nishikawa, M. *Bull. Chem. Soc. Jpn.* **1986**, *59*, 2861.
(6) Cesarano, J., III; Aksay, I. A. *J. Am. Ceram. Soc.* **1988**, *71*, 1062.
(7) Margolin, A.; Sherstyuk, S. F.; Izumrudov, V. A.; Zezin, A. B.; Kabanov, V. A. *Eur. J. Biochem.* **1985**, *146*, 625.
(8) Clark, K. M.; Glatz, C. E. *Biotechnol. Prog.* **1987**, *3*, 241.
(9) Fisher, R. R.; Glatz, C. E. *Biotechnol. Bioeng.* **1988**, *32*, 777.
(10) Bozzano, A. G.; Andrea, G.; Glatz, C. E. *J. Membr. Sci.* **1991**, *55*, 181.
(11) Dubin, P. L.; Strege, M. A.; West, J. In *Large Scale Protein Purification*; Ladish, M., Ed.; American Chemical Society: Washington, DC, 1990; Chapter 5.
(12) von Hippel, P. H.; Bear, D. G.; Morgan, W. D.; McSwiggen, J. A. *Annu. Rev. Biochem.* **1984**, *53*, 389.
(13) Chu, D.; Thomas, J. K. *J. Am. Chem. Soc.* **1986**, *108*, 6270.
(14) Goddard, E. D.; Phillips, T. S.; Hannan, R. B. *J. Soc. Cosmet. Chem.* **1975**, *26*, 461.
(15) Goddard, E. D.; Hannan, R. B. *J. Colloid Interface Sci.* **1976**, *55*, 73.
(16) Goddard, E. D.; Hannan, R. B. *J. Am. Oil Chem. Soc.* **1977**, *54*, 561.
(17) Thalberg, K.; Lindman, B. *J. Phys. Chem.* **1989**, *93*, 1478.
(18) Thalberg, K.; Lindman, B.; Karlström, G. *J. Phys. Chem.* **1990**, *94*, 4289.
(19) Thalberg, K.; Lindman, B.; Karlström, G. *J. Phys. Chem.* **1991**, *95*, 6004.
(20) Thalberg, K.; Lindman, B.; Karlström, G. *J. Phys. Chem.* **1991**, *95*, 3370.
(21) Thalberg, K.; Lindman, B.; Bergfeldt, K. *Langmuir* **1991**, *7*, 2893.
(22) Harada, A.; Nozakura, S. *Polym. Bull.* **1984**, *11*, 175.
(23) Dubin, P. L.; Oteri, R. *J. Colloid Interface Sci.* **1983**, *95*, 453.
(24) Dubin, P. L.; Thé, S. S.; McQuigg, D. W.; Chew, C. H.; Gan, L.-M. *Langmuir* **1989**, *5*, 89.
(25) Dubin, P. L.; Vea, M. E.; Fallon, M. A.; Thé, S. S.; Rigsbee, D. R.; Gan, L.-M. *Langmuir* **1990**, *6*, 1422.
(26) Sudbeck, E. A.; Dubin, P. L.; Curran, M. E.; Skelton, J. *J. Colloid Interface Sci.* **1991**, *142*, 512.
(27) Xia, J.; Zhang, H.; Rigsbee, D. R.; Dubin, P. L.; Shaikh, T. *Macromolecules* **1993**, *26*, 2759.
(28) Chu, B. *Laser Light Scattering*; Academic Press: New York, 1991.
(29) Provencher, S. W. *J. Chem. Phys.* **1976**, *64*, 2772; *Makromol. Chem.* **1979**, *180*, 201.
(30) Ware, B.; Haas, D. D. In *Fast Methods in Physical Biochemistry and Cell Biology*; Sha'afi, R. I., Fernandez, S. M., Eds.; Elsevier: Amsterdam, The Netherlands, 1983; Chapter 8.
(31) Piculell, B.; Lindman, B. *Adv. Colloid Interface Sci.* **1992**, *41*, 149.
(32) Li, Y.; Xia, J.; Dubin, P. L. *Macromolecules*, accepted.

MA9450851